

# Reduced dose CT with model-based iterative reconstruction compared to standard dose CT of the chest, abdomen, and pelvis in oncology patients: intra-individual comparison study on image quality and lesion conspicuity

Linda Nayeli Morimoto,<sup>1</sup> Aya Kamaya,<sup>1</sup> Isabelle Boulay-Coletta,<sup>1,2</sup>  
Dominik Fleischmann,<sup>1</sup> Lior Molvin,<sup>1</sup> Lu Tian,<sup>3</sup> George Fisher,<sup>4</sup> Jia Wang,<sup>5</sup>  
Jürgen K. Willmann<sup>1</sup>

<sup>1</sup>Molecular Imaging Program at Stanford, Department of Radiology, School of Medicine, Stanford University, 300 Pasteur Drive, Room H1307, Stanford, CA 94305-5621, USA

<sup>2</sup>Department of Radiology, Fondation Hôpital Saint-Joseph, Paris, France

<sup>3</sup>Department of Health, Research & Policy, Stanford University, Stanford, CA, USA

<sup>4</sup>Division of Oncology, Department of Medicine, Stanford University, Stanford, CA, USA

<sup>5</sup>Department of Environmental Health and Safety, Stanford University, Stanford, CA, USA

## Abstract

**Purpose:** To compare image quality and lesion conspicuity of reduced dose (RD) CT with model-based iterative reconstruction (MBIR) compared to standard dose (SD) CT in patients undergoing oncological follow-up imaging.

**Methods:** Forty-four cancer patients who had a staging SD CT within 12 months were prospectively included to undergo a weight-based RD CT with MBIR. Radiation dose was recorded and tissue attenuation and image noise of four tissue types were measured. Reproducibility of target lesion size measurements of up to 5 target lesions per patient were analyzed. Subjective image quality was evaluated for three readers independently utilizing 4- or 5-point Likert scales.

**Results:** Median radiation dose reduction was 46% using RD CT ( $P < 0.01$ ). Median image noise across all measured tissue types was lower ( $P < 0.01$ ) in RD CT. Subjective image quality for RD CT was higher ( $P < 0.01$ ) in regard to image noise and overall image

quality; however, there was no statistically significant difference regarding image sharpness ( $P = 0.59$ ). There were subjectively more artifacts on RD CT ( $P < 0.01$ ). Lesion conspicuity was subjectively better in RD CT ( $P < 0.01$ ). Repeated target lesion size measurements were highly reproducible both on SD CT (ICC = 0.987) and RD CT (ICC = 0.97).

**Conclusions:** RD CT imaging with MBIR provides diagnostic imaging quality and comparable lesion conspicuity on follow-up exams while allowing dose reduction by a median of 46% compared to SD CT imaging.

**Key words:** Radiation dose reduction—Image noise—Computer tomography—Cancer—Model-based iterative reconstruction (MBIR)

Computed tomography (CT) imaging is fast, reliable, and widely available, and thus is routinely used for diagnosis, staging, treatment response assessment, and surveillance in oncology [1–3]. As usage of CT imaging has become more prevalent, radiation exposure has increased and dose-decreasing strategies are becoming more warranted [4, 5]. While attempts to reduce radiation exposure are generally commendable, this should

This manuscript was presented at RSNA 2015. Results were presented as an oral talk at SAR 2014.

Correspondence to: Jürgen K. Willmann; email: willmann@stanford.edu

not come at the risk of decreasing image quality and diagnostic accuracy [6]. Several dose reduction techniques have been introduced in the last decade, such as helical acquisition, adaptive section collimation, tube current modulation, automatic exposure control, peak kilovoltage adjustment, and adaptive noise reduction filters [7, 8], which are routinely implemented on state-of-the-art CT equipment.

A newer approach is to tackle the reconstruction process of the image data. Filtered back projection (FBP) had been the most frequently used technique and is considered the reference standard. However, it relies on the relationship between the measured attenuation and the pixel values in the image and assumes that these measurements are truly reflective of the actual data values [9]. In reality, the data are noisy and the noise is subsequently amplified [9]. Newer technologies involve the use of iterative reconstruction (IR) which statistically models the object, noise, and CT imaging system itself in the projection data with forward (projection data generated from the images) and backward (images reconstructed from the projected data) reconstruction steps [10, 11]. Adaptive statistical iterative reconstruction (ASIR) was developed as one type of first generation iterative reconstruction algorithm, capable of dose reduction over a wide range. In clinical practice, ASIR is utilized as a hybrid technique with FBP and images are blended to obtain combined images [11] with vendor recommended dose reduction ranging between 30 and 50% [12].

A next generation full IR algorithm, model-based iterative reconstruction (MBIR), also takes into account system statistics and system optics and further reduces image noise at reduced dose settings [11]. As a full IR technique, MBIR performs multiple backwards and forwards reconstructions, without the need to blend with FBP [11]. Advantages are that it produces better image quality than FBP at very low signal-to-noise ratio settings [9] and low-radiation dose settings while maintaining high spatial resolution [13].

Previous studies have compared image quality of low-dose datasets reconstructed by FBP, ASIR, or MBIR obtained from various organs such as the liver [3, 10, 14, 15], small bowel [16], colon [17], and lungs [18–23]. They showed that low-dose techniques with IR are feasible, thereby allowing decreased radiation dose while gaining more contrast to noise, less noise, and improved lesion or structural conspicuity. However, there is little experience regarding objective and subjective image quality of CT images reconstructed by MBIR versus the current standard of care reconstructions (FBP/FBP–ASIR blend) in an intra-individual prospective comparison study in cancer patients [24]. The cancer patient population is a good surrogate to compare the effects of radiation dose reduction on image quality as patients undergo multiple exams.

Therefore, the purpose of this intra-individual prospective comparison study was to compare image quality and lesion conspicuity of reduced dose (RD) CT with MBIR compared to standard dose (SD) CT in patients undergoing oncological follow-up imaging.

## Materials and methods

### Patients

This HIPPA compliant prospective study was approved by the Institutional Review Board of our institution and written consent was obtained from all participating patients. One radiologist reviewed the daily list of patients scheduled for CT imaging between a 6-month period. Patients over 18 years old with a known diagnosis of cancer who presented for a routine scheduled follow-up single contrast phase chest, abdomen, and pelvis CT examination were screened for possible inclusion. Only those patients with at least one routine single contrast phase chest, abdomen, and pelvis CT examination performed in our institution within the last 12 months were considered for possible inclusion. Consecutive eligible patients were selected randomly with a maximum of two patients included daily to avoid delays in clinical workflow due to the long reconstruction times of MBIR [15, 25, 26].

Patients who were unable to provide written informed consent or could not obtain intravenous contrast due to major contrast agent allergy or compromised renal function defined as a creatinine of greater than 1.5 were excluded. Seventy-six patients met the study inclusion criteria. Thirty-two patients (41%) were excluded (Fig. 1). The final study population consisted of 44 patients (19 women and 25 men; mean age, 58.6 years; range, 33–85 years). A subset of the included patients, 35

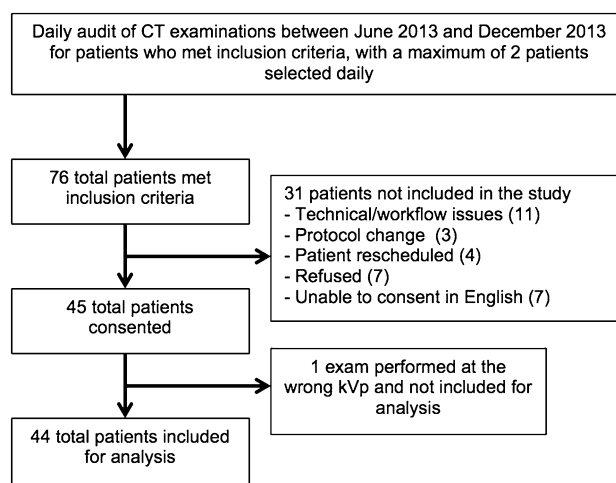


Fig. 1. Flowchart of the patient selection process.

in total, had a total of 138 target lesions included for analysis of lesion size and lesion conspicuity.

For each patient, weight (mean, 77 kg; range, 45–122 kg) was recorded. Prior weight was retrospectively obtained from the patient chart (mean, 79 kg; range, 45–122 kg). This difference in patients' weights at the two time points was small but statistically significant (median, 0.7 kg; 95% CI 0–2.3 kg;  $P = 0.03$ ). The average time interval between previous SD CT and RD CT scans was 106 days (range, 28–365 days).

The majority of patients carried a diagnosis of colorectal carcinoma ( $n = 12$ ), lymphoma ( $n = 7$ ), lung cancer ( $n = 6$ ), or breast cancer ( $n = 5$ ). Other cancer indications included gastric cancer ( $n = 3$ ), pancreatic cancer ( $n = 3$ ), small bowel cancer ( $n = 2$ ), head and neck cancers ( $n = 2$ ), ovarian cancer ( $n = 2$ ), esophageal cancer ( $n = 1$ ), and prostate cancer ( $n = 1$ ).

### Standard dose routine multi-detector row CT imaging technique

All patients had previously undergone a routine standard dose (SD), single-phase chest, abdomen, and pelvis CT on one of six multi-detector row CT scanners at our institution. Reconstruction technique, scanning parameters, and number of patients scanned on each of these CT scanners are listed in Table 1. Automated tube current modulation was used on all acquisitions: CarekV and CareDose 4D (Siemens) were used with a Reference tube voltage of 120 kV and Quality Reference mAs of 200. Smart mA (GE) technique was used with the noise index (NI) adjusted to patient weight and for a reconstruction slice thickness of 0.625 mm. Due to differences in automated exposure control software versions, the numerical values of NI tables varied across different GE scanners based on three weight categories. The NI values ranged from 46 for patients greater than 91 kg, 37 for patients between 68 and 91 kg, and 30 for patients less than 68 kg on the Discovery HD750 (GE) to 37, 29, and 24,

respectively, for the Discovery 690 (GE) and Lightspeed VCT (GE). For chest imaging, the “B45f” convolution kernel (Siemens) and the “Bone” convolution kernel (GE) was used. For abdomen and pelvis imaging, the “B20f” (Siemens) kernel and the “Soft” convolution kernel (GE) was. All datasets were reformatted to a transverse slice thickness of 1.0 mm (Siemens), or 1.25 mm (GE). The transverse images were subsequently used for both quantitative and qualitative image analysis.

### Reduced dose multi-detector row CT imaging technique

All patients were scanned on an outpatient clinic 64-detector row CT scanner (Discovery 750HD, GE Healthcare, Milwaukee, WI) using the following parameters: 0.625-mm collimation, 100 kilovolt peak (kVp), and automated milliamperage modulation (Smart mA, GE Healthcare). The following parameters varied based on established institutional guideline tables followed by the technologists to optimize image quality based on patient body weight: pitch (either 0.5156 or 1.375) and gantry rotation time (mean, 0.8 s; range, 0.4–1.0 s). All patients were assigned one of three NI values based on their weight. To target a 50% dose reduction at 0.625-mm slice thickness, a NI value of 72 was selected for patients over 91 kg, a value of 51 for patients between 68 and 91 kg, and a value of 43 for patients less than 68 kg. Axial images at 0.625 mm were acquired and image reconstruction was performed with MBIR (Veo 1.0, GE Healthcare). These were further reformatted to obtain axial 1.0–1.3 mm slices of the chest, abdomen, and pelvis. These images were subsequently used for quantitative and qualitative image analysis (Fig. 2).

For both SD and RD CT scans, a weight-based amount of iodinated contrast medium, at 1.6 mL/kg at 350–370 mgI/mL, was injected over 40 s using a power injector (Empower CTA, E-Z-EM Inc., Westbury, NY, USA). Timing for portal venous phase was obtained by

**Table 1.** Summary of prior standard dose CT scan parameters

| CT scanner                       | Reconstruction algorithm | Detector collimation (mm) | Ref kV/QRM or NI     | kVP | Number of patients |
|----------------------------------|--------------------------|---------------------------|----------------------|-----|--------------------|
| Siemens SOMATOM Definition DS    | FBP                      | 32 × 0.6                  | 120/200 <sup>c</sup> | 100 | 9                  |
|                                  |                          |                           |                      | 120 | 2                  |
| Siemens SOMATOM Definition AS+   | FBP                      | 64 × 0.6                  | 100/276 <sup>d</sup> | 100 | 4                  |
| Siemens SOMATOM Sensation 64     | FBP                      | 64 × 0.6                  | 120/200              | 120 | 11                 |
| GE Lightspeed VCT <sup>a</sup>   | ASIR/FBP <sup>b</sup>    | 64 × 0.625                | 24                   | 120 | 1                  |
| GE Discovery 690 <sup>a</sup>    | FBP                      | 64 × 0.625                | 11.5                 | 120 | 1                  |
| GE Discovery 750 HD <sup>a</sup> | ASIR/FBP <sup>b</sup>    | 64 × 0.625                | 30–54                | 80  | 1                  |
|                                  |                          |                           |                      | 100 | 8                  |
|                                  |                          |                           |                      | 120 | 7                  |

FBP Filtered back projection, ASIR adaptive statistical iterative reconstruction, ref kV reference kilovolt, QRM quality reference mAs (for Siemens scanners), NI noise index (for GE scanners)

<sup>a</sup> For all GE scanners, reference slice thickness for Noise Index is 0.625 mm

<sup>b</sup> For patients with ASIR/FBP, the chest was reconstructed with 30% ASIR/70% FBP and the abdomen and pelvis were reconstructed with 40% ASIR/60% FBP, per standard institutional protocol

<sup>c</sup> One patient scanned at 120 kVp and QRM of 250 and another at 100 kV and QRM of 350 because of large patient size

<sup>d</sup> One patient scanned at 100 kVp and QRM of 344 because of large patient size

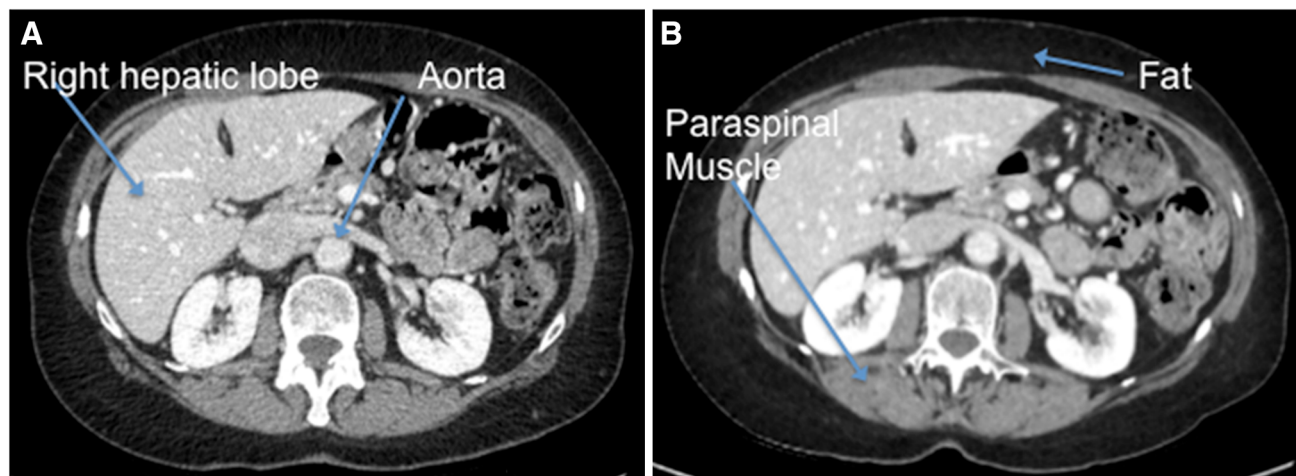


**Fig. 2.** A 51-year-old female with rectal carcinoma scanned with SD and RD CT scans, 119 days apart. Transverse contrast-enhanced SD with 40% ASIR (**A**) and RD with MBIR (**B**) CT scans at the level of the left renal vein show the four

tissue types examined for quantitative noise measurements: right hepatic lobe, aorta, right paraspinal muscle, and anterior subcutaneous fat.

use of an empirical 65-s delay after the start of the contrast injection.

### Quantitative image analysis

Quantitative image analysis of all CT datasets (SD and RD data) was performed by one board certified, body fellowship-trained radiologist with 6 years of experience in oncologic CT imaging. Quantitative imaging data analysis included recording of the radiation dose, quantitative assessment of image noise, and measurement of the maximal diameter of up to 5 target lesions according to response evaluation criteria in solid tumors (RECIST) 1.1 [27, 28].

### Radiation dose

The  $CTDI_{vol}$  values for the SD and RD CT scans recorded for all acquisitions were retrieved from the dose reports generated by the CT scanners and archived on the picture archiving and communications system (PACS, GE Healthcare). The average percentage dose reduction per patient was calculated based on the difference between the  $CTDI_{vol}$  of the SD versus the RD CT scan  $[(RD\ MBIR\ CTDI_{vol} - SD\ CTDI_{vol})/SD\ CTDI_{vol}] \times 100\%$ .

### Image noise

Noise values (standard deviations in Hounsfield units) were measured by drawing a circular region of interest (ROI) measuring  $50\ mm^2$  on transverse images of both the SD and RD CT scans in the following four predetermined anatomical sites as described [3, 26, 29, 30], all obtained at the level of the left renal vein: (1), in the anterior abdominal wall fat; (2), in the lumen of the

abdominal aorta; (3), in the right hepatic lobe parenchyma; and (4), in the right paraspinal musculature. Gross visible tissue inhomogeneities such as vessels or dilated bile ducts in the liver parenchyma, atherosclerotic plaques of the aorta, or striations of fat in the paraspinal musculature, if present, were avoided in the ROI.

### Maximal lesion diameter measurements

Up to five index lesions were found in patients with target lesions and the maximum diameter was measured on transverse images on both SD and RD CT scans. All lesions were re-measured at least 3 weeks later by the same reader to assess reproducibility of index lesion measurements.

### Qualitative image analysis

Qualitative image analysis was performed by three board-certified, fellowship-trained body radiologists (reader A, 22 years; reader B, 14 years; and reader C, 6 years of experience in CT cancer imaging). All readers were blinded to patient demographic information, history, diagnosis, and imaging findings. After an initial training session with three randomly selected MBIR studies which were not part of this study in order to familiarize all readers with the criteria used for qualitative image analysis, all readers independently analyzed the transverse SD and RD CT scans in randomized fashion on a dedicated two-monitor PACS workstation (Coronis 3 MP (MDCG 3120), Barco, Inc., Barco NV, Belgium). Transverse images were initially presented in standard soft tissue windows (window width, 320; window length, 50) and readers were encouraged to change window settings and zoom images as they deemed nec-



essary. Scoring sheets were provided to the readers to grade the following parameters by using Likert grading scales: Image contrast, subjective image noise, artifacts, overall subjective image quality, and lesion conspicuity.

#### *Image contrast*

Image contrast scoring of grade 1 (excellent), 2 (good), 3 (moderate), 4 (suboptimal), and 5 (poor) was based upon the ability to visualize small anatomic structures on transverse images. Within the chest, images were evaluated to determine whether pulmonary vessels were visible within 1 cm of the pleura and if both internal mammary arteries were visualized in at least 75% of their course [12, 19, 31]. Within the abdomen and pelvis, visibility of the following three anatomical structures was assessed: subsegmental portal vein branches to within 2 cm of the capsule, entire course of the common bile duct, and at least 75% of the course of the non-opacified ureters [32, 33]. If all structures were seen, this was scored as grade 1, excellent. If one structure was lacking, this would be scored as grade 2, good; if two structures were lacking, this would be scored as grade 3, moderate. A grade 4, suboptimal and a grade 5, poor were reserved for studies with three or four or more structures not visible, respectively.

#### *Subjective image noise*

Image noise was graded on a five-point scale based on the overall perception of quantum mottling in the images [3], defined as the readers' perceptions of the graininess to the images compared to what the reader is used to on average CT scans. This was graded as 1, minimal; 2, less than average; 3, average; 4, above average; and 5, unacceptable.

#### *Artifacts*

Artifacts were graded on a four-point scale: grade 1, no artifacts; grade 2, some artifact present not affecting interpretation; grade 3, artifacts present affecting interpretation but still diagnostic; and grade 4, artifacts present affecting interpretation and not diagnostic. Readers were also asked to list the type of artifacts noticed as follows: streak artifact (from hardware or vessels), pixelation (a step-wise artifact at tissue interfaces), or beam hardening [3, 25, 31].

#### *Overall subjective image quality*

Overall subjective image quality was scored on a four-point scale: grade 1, "better than what I am used to and diagnostic"; grade 2, "similar to what I am used to and diagnostic"; grade 3, "worse than what I am used to but still diagnostic"; and grade 4, "worse than what I am used to and not diagnostic."

#### *Lesion conspicuity*

Lesion conspicuity was scored using a three-point Likert scale. Lesions that completely resolved in the interval or patients without index lesions were not included for analysis. The preselected lesions were marked and bookmarked on PACS by the same reader who measured the diameter of the target lesions. All readers were provided a list of accession numbers and instructed to choose a numbered bookmark that contained the preselected target lesions. Conspicuity of each lesion was evaluated using the following grading scale: grade 1, "lesion delineation against the surrounding tissue is better than what I am used to"; grade 2, "lesion delineation against the surrounding tissue is similar to what I am used to"; and grade 3, "lesion delineation against the surrounding tissue is worse than what I am used to." This was performed for both the SD and RD CT scans.

#### *Statistical analysis*

The sample size of 44 patients was chosen for the study to have 80% power for detecting a mean difference of 0.45 standard deviation with the paired Wilcoxon rank sum test at the significance level of 0.05 and we hypothesized that the differences in relevant parameters of RD CT with MBIR and the standard of care SD CT are greater than 0.45 standard deviation.

Radiation dose reductions were summarized with median levels and 95% confidence intervals (CI). Quantitative noise reduction and Hounsfield Unit attenuation were summarized with their median levels and 95% CI by different tissue types. The *P* values between SD and RD CT were obtained with non-parametric Wilcoxon test. The trend test was performed to test the association between the dose reduction and baseline weight. The reproducibility of maximal diameter measurements of target lesions on both SD and RD CT images were measured with the estimated intraclass correlation coefficients (ICC) and the corresponding 95% CI based on bootstrap method. For comparing qualitative image measurements including image contrast, image noise, overall image quality, artifacts, and lesion conspicuity, the non-parametric paired sign test was performed for each reader separately. All statistical tests were two-sided with a significance level of 0.05. The statistical analysis was performed using R. 3.1.3 (R foundations for statistical computing).

## **Results**

### *Quantitative image analysis*

#### *Radiation dose reduction*

Radiation dose was significantly reduced ( $P < 0.001$ ) by a median of 46.2% (95% CI 40.7–49.2%; range, 6.3–68.8%) with RD compared to SD imaging ( $\text{CTDI}_{\text{vol}}$ :

**Table 2.** Median radiation dose reduction among the three patient weight categories

| Number   | Weight category (kg) | Weight range (kg) | Median CTDI <sub>vol</sub> radiation dose SD CT (mGy) | Median CTDI <sub>vol</sub> radiation dose RD CT (mGy) | Median percent reduction (%) |
|----------|----------------------|-------------------|---|---|------------------------------|
| 18       | <68                  | 44.9–65.8         | 10.9  | 5.6   | 47.8                         |
| 15       | 68–91                | 69.4–88.4         | 15.0  | 7.8   | 46.1                         |
| 11       | >91                  | 93.0–122.5        | 19.2  | 9.7   | 38.7                         |
| Total 44 |                      |                   | 13.0  | 7.3   | 46.2                         |

CTDI<sub>vol</sub> CT dose index volume, SD standard dose, RD reduced dose

7.3 ± 3.4 vs. 13.0 ± 4.5 mGy, respectively, DLP: 520.5 ± 240.2 vs. 864.5 ± 334.8 mGy cm). The median dose reduction was 38.7% (95% CI 23.5–68.8%) in patients >91 kg, 46.1% (95% CI 39.2–49.2%) in patients between 68 and 91 kg, and 47.8% (95% CI 36.4–56.1%) in patients <68 kg (Table 2). There was no statistically significant difference ( $P = 0.624$ ) in dose reduction among the three different weight classes.

#### Quantitative image noise

Median image noise was significantly lower on RD versus SD CT images across all tissues measured ( $P < 0.001$ ; Table 3). Whereas the median reduction of image noise obtained on RD CT compared to SD CT was approximately 50% in the abdominal aorta (54.5%, 95% CI 49.6–58.1%), right hepatic lobe (49.4%, 95% CI 44.8–55.8%), and paraspinal musculature (50.2%, 95% CI 40.7–55.1%), the noise reduction was less in anterior abdominal fat with a median reduction of 33.1% (95% CI 24.2–41.7%); however, noise reduction was still statistically significant ( $P < 0.001$ ) in abdominal fat. Hounsfield Unit attenuation per tissue type also varied significantly ( $P < 0.001$ ) across all tissue types when comparing RD images to SD images with the Hounsfield Unit attenuation measuring higher on average in the aorta, liver, and paraspinal musculature and lower in fat (Table 4).

#### Reproducibility of maximal lesion diameter measurements

Of the 138 target lesions included for analysis that were subsequently evaluated on both RD and SD CT imaging, there were 70 lymph nodes (range 3–23 mm), 31 lung

lesions (range 3–88 mm), 13 liver lesions (range 4–65 mm), 8 abdominopelvic implants (range 8–36 mm), 6 adrenal lesions (range 13–50 mm), 3 bowel masses (range 13–48 mm), 3 pancreatic lesions (range 17–30 mm), 3 muscle lesions (range 13–38 mm), and 1 osseous lesion (range 19–25 mm).

There was excellent reproducibility of maximal diameter measurements of the analyzed lesions on both RD and SD CT images. The intraclass correlation coefficient was 0.982 (95% CI 0.971, 0.989) for measurements obtained on RD and 0.987 (95% CI 0.979, 0.992) on SD CT images.

#### Qualitative image analysis

##### Image contrast

Overall, all three readers noted that the ability to visualize the small anatomic structures of interest was good to excellent on both RD and SD CT images and there was no statistically significant difference ( $P = 0.59$ ) between RD and SD CT images in terms of image contrast (Table 5).

##### Subjective image noise

Overall, there was noted to be significantly ( $P < 0.01$ ) lower noise on RD compared to SD CT images (Table 5) although one reader (Reader B) favored SD CT over RD CT ( $P < 0.01$ ).

##### Artifacts

Artifacts were significantly more often noted on RD compared to SD CT ( $P < 0.01$ ; Table 5). The vast

**Table 3.** Median noise and percent noise reduction per tissue type

| Tissue type | SD CT             |            | RD CT             |            | Percent change |                |
|-------------|-------------------|------------|-------------------|------------|----------------|----------------|
|             | Median noise (HU) | Range (HU) | Median noise (HU) | Range (HU) | Median (%)     | Range (%)      |
| Fat         | 16.4              | 8.8–32.4   | 11.1              | 6.7–20.7   | 33.1           | –84.1 to –77.5 |
| Aorta       | 28.2              | 15.4–52.4  | 13.5              | 7.7–20.4   | 54.5           | –1.9 to –73.5  |
| Liver       | 20.7              | 12.5–52.4  | 10.8              | 6.5–18.5   | 49.4           | –6.4 to –78.7  |
| Muscle      | 21.5              | 13.1–44.4  | 11.3              | 7.1–17.8   | 50.2           | 0 to –78.9     |

SD Standard dose, RD reduced dose, HU hounsfield unit

**Table 4.** Median attenuation measurements per tissue type

| Tissue type | Median SD CT attenuation (HU) | Median RD CT attenuation (HU) | Median percent change (%) | Confidence interval (%) |
|-------------|-------------------------------|-------------------------------|---------------------------|-------------------------|
| Fat         | -105.5                        | -117.6                        | 12.4                      | 7.2–17.0                |
| Aorta       | 171.7                         | 197.6                         | 14.3                      | 2.1–21/3                |
| Liver       | 108.5                         | 137.1                         | 20.4                      | 12.0–28.4               |
| Muscle      | 57.6                          | 60.8                          | 6.8                       | 0.0–16.2                |

SD Standard dose, RD reduced dose, HU hounsfield unit

majority of artifacts were graded as “some artifact present not affecting interpretation” (a grade of 2).

#### Overall subjective image quality

Overall subjective image quality was significantly higher ( $P < 0.01$ ) on RD compared to SD CT images when taken in total (Table 5). Reader A graded the quality between SD CT and RD CT as fairly comparable with most RD CT cases and SD CT cases graded as “similar to what I am used to and diagnostic.” Although Reader B also graded most cases as “similar to what I am used to and diagnostic” for both RD CT and SD CT, there was significantly better ( $P < 0.01$ ) overall subjective image quality in favor of SD CT. Reader C, however, graded overall image quality of RD CT images significantly higher than SD CT images ( $P < 0.01$ ).

#### Lesion conspicuity

Overall, lesion conspicuity was graded significantly ( $P < 0.01$ ) higher on RD CT images compared to SD CT images (Table 5), although one reader (Reader C) graded RD CT and SD CT similarly ( $P = 0.32$ ). In general, conspicuity of most target lesions was graded as grade 2 (“lesion delineation against the surrounding tissue is similar to what I am used to”) on RD CT images.

## Discussion

This study showed that RD CT with MBIR maintains image quality compared to our institution’s current standard of care SD CT while reducing the median dose by nearly half in follow-up oncology patients. For three independent readers, subjective image quality assessments were graded substantially higher and image noise substantially lower on RD compared to SD CT exams. Also, dose reduction did not compromise reproducibility of consecutive target lesion size measurements, suggesting that this technique can be used for routine follow-up imaging in cancer patients.

The NI values used in this study were selected based on our previous experience with in house phantom testing and an independent group of 30 consecutive patients (data not shown and not part of this study) for which radiation dose at acceptable image quality was optimized for the three weight classes for routine clinical purposes in our institution. The chosen NI values were selected to

target a dose that was approximately half of what the expected  $CTDI_{vol}$  would have been for a SD CT exam of patients in these three weight classes. A target of ~50% dose reduction was considered realistic as previous studies reported that image quality using MBIR at this dose reduction level was still acceptable [3, 34]. Further reduction of dose resulted in perceived non-diagnostic image quality of the kidneys and retroperitoneum in a different study analyzing imaging quality of MBIR reconstructed excretory phase CT datasets at different dose reduction levels [34]. Compared to other studies, in our study we did not use a fixed NI for RD CT scans for all patients, but rather introduced a strategy with three noise values associated with different weight categories. With this strategy we were accepting higher NI for more obese patients, thereby also allowing substantial dose reduction in that patient group despite automatic upregulation of the tube current by the CT scanner. Consequently, there was no significant difference in dose reduction among the three patient weight groups.

Previous studies assessed objective and subjective image quality criteria on RD datasets reconstructed with different reconstruction algorithms such as FBP, ASIR, and MBIR in several body parts [3, 10, 14–23]. In those studies, MBIR outperformed FBP and ASIR in terms of diagnostic image quality when applied to RD CT datasets due to its more complex and accurate reconstruction algorithm. Our study expands previous reports by using a different study design exploring the performance of MBIR in an intra-individual comparison study of consecutive cancer patients scanned with RD CT and using their previous SD CT scans as intra-individual control exams. The results of our study confirmed our hypothesis that for the purpose of oncological follow-up exams, MBIR allows substantially reduced radiation dose of chest, abdomen, and pelvic CT scans while maintaining diagnostic imaging quality. Interestingly, although readers noted that MBIR reconstructed datasets often appeared “blurry” in our study, also sometimes referred to as “pixelated blotchy artifact” [35], all three readers, in particular reader C, rated overall subjective image quality of MBIR datasets equal to or higher than standard of care SD CT scans. While there are several factors influencing radiologists’ perceptions of image quality, based on our experience with MBIR, some of this is related to becoming accustomed to the different looks of CT scans over time and appreciating the objectively de-

**Table 5.** Summary of subjective image quality numerical scores per reader for all examined categories of qualitative image analysis comparing standard dose and reduced dose CT

| Score                            | Reader A |       | Reader B |       | Reader C |       | Combined <i>P</i> values |
|----------------------------------|----------|-------|----------|-------|----------|-------|--------------------------|
|                                  | SD CT    | RD CT | SD CT    | RD CT | SD CT    | RD CT |                          |
| Image contrast                   |          |       |          |       |          |       |                          |
| 1                                | 36       | 37    | 37       | 37    | 28       | 32    | 0.59                     |
| 2                                | 6        | 7     | 6        | 6     | 6        | 4     |                          |
| 3                                | 2        | 0     | 1        | 1     | 9        | 5     |                          |
| 4                                | 0        | 0     | 0        | 0     | 1        | 3     |                          |
| 5                                | 0        | 0     | 0        | 0     | 0        | 0     |                          |
| Mean                             | 1.2      | 1.2   | 1.2      | 1.2   | 1.6      | 1.5   |                          |
| <i>P</i> value                   | 0.75     |       | 1.0      |       | 0.52     |       |                          |
| Image noise                      |          |       |          |       |          |       |                          |
| 1                                | 0        | 11    | 9        | 4     | 1        | 24    | <0.01                    |
| 2                                | 8        | 29    | 20       | 15    | 6        | 16    |                          |
| 3                                | 33       | 4     | 12       | 21    | 31       | 4     |                          |
| 4                                | 3        | 0     | 3        | 4     | 6        | 0     |                          |
| 5                                | 0        | 0     | 0        | 0     | 0        | 0     |                          |
| Mean                             | 2.9      | 1.8   | 2.2      | 2.6   | 3.0      | 1.5   |                          |
| <i>P</i> value                   | <0.01    |       | <0.01*   |       | <0.01    |       |                          |
| Artifacts                        |          |       |          |       |          |       |                          |
| 1                                | 13       | 8     | 33       | 19    | 18       | 14    | <0.01                    |
| 2                                | 28       | 35    | 11       | 24    | 25       | 29    |                          |
| 3                                | 1        | 1     | 0        | 1     | 1        | 1     |                          |
| 4                                | 2        | 0     | 0        | 0     | 0        | 0     |                          |
| Mean                             | 1.8      | 1.8   | 1.3      | 1.6   | 1.6      | 1.7   |                          |
| <i>P</i> value                   | 0.61     |       | <0.01    |       | 0.54     |       |                          |
| Overall subjective image quality |          |       |          |       |          |       |                          |
| 1                                | 0        | 3     | 10       | 0     | 0        | 36    | <0.01                    |
| 2                                | 41       | 35    | 28       | 35    | 39       | 6     |                          |
| 3                                | 3        | 6     | 6        | 8     | 5        | 2     |                          |
| 4                                | 0        | 0     | 0        | 1     | 0        | 0     |                          |
| Mean                             | 2.1      | 2.1   | 1.9      | 2.2   | 2.1      | 1.2   |                          |
| <i>P</i> value                   | 1.0      |       | <0.01*   |       | <0.01    |       |                          |
| Lesion conspicuity               |          |       |          |       |          |       |                          |
| 1                                |          | 9     | 2        | 23    | 0        | 0     | <0.01                    |
| 2                                | 129      | 126   | 124      | 104   | 112      | 117   |                          |
| 3                                | 8        | 3     | 11       | 11    | 26       | 21    |                          |
| Mean                             | 2.1      | 2.0   | 2.1      | 1.9   | 2.2      | 2.2   |                          |
| <i>P</i> value                   | <0.01    |       | <0.01    |       | 0.32     |       |                          |

SD Standard dose, RD reduced dose, HU hounsfield unit

\* SD CT favored over RD CT

creased noise following iterative reconstruction of the CT datasets.

We acknowledge the following limitations of our study. First, this study did not address how accurate the interpretation of the CT exam was regarding cancer detection and staging. Rather, this study addressed whether image quality on RD CT scans was sufficiently high in patients with known cancer to monitor their disease. More studies are warranted to address how the use of MBIR in RD CT exams may affect other aspects of diagnostic imaging such as in characterizing focal lesions. In fact, our study showed that there were substantial differences in HU attenuation measurements in the tissues measured between the RD and SD images, confirming previous reports [3, 32, 36] and indicating that the use of MBIR may affect interpretation of entities based on absolute HU value measurements or analysis of other quantitative CT features [37]. Second, the nature of our study design introduces the potential limitation that lesion conspicuity may change in patients undergoing

cancer treatment due to the course of treatment or course of disease rather than CT reconstruction technique as the lesions grew or got smaller in the time interval. Lesion conspicuity could both increase or decrease in our population and both progression and improvement could occur. However, it is unlikely that this limits the generalizability of these results. Third, the prospectively implemented dose reduction protocol using MBIR in this study was compared with various standard dose routine protocols implemented on a total of six different CT scanners available in our institution at the time of the study. Automatic exposure control dependence on patient size varied among different scanner models, therefore, although we reconciled dose performance and image quality on different scanners for an average adult patient size, the actual dose and resultant image quality varied due to different automatic exposure control behaviors. However, we chose this study design to reflect a real-life setting of an institution running several types of CT scanners with different protocols which improves



generalizability of our results. Finally, since reconstruction times of the MBIR technique used in our study were long (averaging ~120 min, though this was not systematically measured as part of our study), this limited the inclusion of patients to a maximum two per day to not interfere with routine clinical workflow and may have biased patient inclusion in our study. MBIR incorporates the geometry of the whole imaging chain, including the finite size of X-ray focal spot size, cone-beam shape, detector elements, and three-dimensional reconstruction voxels [38]. Both photon statistics and electronic noise are modeled in MBIR. The extensive modeling of forward projection process is part of the reason that MBIR takes substantially longer reconstruction time than previous generations of IR techniques, such as ASIR. Further improvements of MBIR and alternative next generation iterative reconstruction algorithms may provide faster data reconstruction allowing larger scale implementation of low-dose strategies in the clinic [39, 40].

In conclusion, our study suggests that RD CT imaging with MBIR allows radiation dose reduction by almost 50% compared to a spectrum of current standard of care SD CT protocols while not interfering with diagnostic image quality. Reduced dose CT protocols using modern reconstruction algorithms may soon become the standard of care and could be expanded to other CT indications beyond cancer imaging.

#### Compliance with ethical standards

**Funding** No funding was received for this study.

**Conflict of interest** Dominik Fleischmann, MD has received research support from Siemens Medical Solutions and General Electric HealthCare and has ownership interest in iSchemaView Inc. Lior Molvin is an imaging consultant for General Electric HealthCare. Jürgen Willmann, MD has no conflicts of interest related to current work; unrelated potential conflicts: Dr. Willmann is in the scientific advisory board of Lantheus, Bracco, and SonoVol; is consultant to Bracco; and receives grant support by Siemens, GE, Bracco, and Philips. The other authors declare that they have no conflict of interest.

**Ethical approval** All procedures performed in studies involving human participants were in accordance with the ethical standards of the institutional and/or national research committee and with the 1964 Helsinki declaration and its later amendments or comparable ethical standards.

**Informed consent** Informed consent was obtained from all individual participants included in the study.

#### References

- Brenner DJ, Hall EJ (2007) Computed tomography—an increasing source of radiation exposure. *N Engl J Med* 357(22):2277–2284. doi:10.1056/NEJMr072149
- Mettler FA Jr, Bhargavan M, Faulkner K, et al. (2009) Radiologic and nuclear medicine studies in the United States and worldwide: frequency, radiation dose, and comparison with other radiation sources—1950–2007. *Radiology* 253(2):520–531. doi:10.1148/radiol.2532082010
- Chang W, Lee JM, Lee K, et al. (2013) Assessment of a model-based, iterative reconstruction algorithm (MBIR) regarding image quality and dose reduction in liver computed tomography. *Invest Radiol* 48(8):598–606. doi:10.1097/RLI.0b013e3182899104
- Initiative to reduce unnecessary radiation exposure from medical imaging (February 2010). Silver Spring, MD
- Amis ES Jr, Butler PF, Applegate KE, et al. (2007) American College of Radiology white paper on radiation dose in medicine. *J Am Coll Radiol* 4(5):272–284. doi:10.1016/j.jacr.2007.03.002
- Yu L, Bruesewitz MR, Thomas KB, et al. (2011) Optimal tube potential for radiation dose reduction in pediatric CT: principles, clinical implementations, and pitfalls. *Radiographics* 31(3):835–848. doi:10.1148/rg.313105079
- Gunn ML, Kohr JR (2010) State of the art: technologies for computed tomography dose reduction. *Emerg Radiol* 17(3):209–218. doi:10.1007/s10140-009-0850-6
- McCullough CH, Bruesewitz MR, Kofler JM Jr (2006) CT dose reduction and dose management tools: overview of available options. *Radiographics* 26(2):503–512. doi:10.1148/rg.262055138
- Fleischmann D, Boas FE (2011) Computed tomography—old ideas and new technology. *Eur Radiol* 21(3):510–517. doi:10.1007/s00330-011-2056-z
- Mitsumori LM, Shuman WP, Busey JM, Kolokythas O, Koprowicz KM (2012) Adaptive statistical iterative reconstruction versus filtered back projection in the same patient: 64 channel liver CT image quality and patient radiation dose. *Eur Radiol* 22(1):138–143. doi:10.1007/s00330-011-2186-3
- Willeminck MJ, de Jong PA, Leiner T, et al. (2013) Iterative reconstruction techniques for computed tomography Part 1: technical principles. *Eur Radiol* 23(6):1623–1631. doi:10.1007/s00330-012-2765-y
- Prakash P, Kalra MK, Digumarthy SR, et al. (2010) Radiation dose reduction with chest computed tomography using adaptive statistical iterative reconstruction technique: initial experience. *J Comput Assist Tomogr* 34(1):40–45. doi:10.1097/RCT.0b013e3181b26c67
- Smith EA, Dillman JR, Goodsitt MM, et al. (2014) Model-based iterative reconstruction: effect on patient radiation dose and image quality in pediatric body CT. *Radiology* 270(2):526–534. doi:10.1148/radiol.13130362
- Shuman WP, Green DE, Busey JM, et al. (2013) Model-based iterative reconstruction versus adaptive statistical iterative reconstruction and filtered back projection in liver 64-MDCT: focal lesion detection, lesion conspicuity, and image noise. *AJR Am J Roentgenol* 200(5):1071–1076. doi:10.2214/AJR.12.8986
- Volders D, Bols A, Haspelslagh M, Coenegrachts K (2013) Model-based iterative reconstruction and adaptive statistical iterative reconstruction techniques in abdominal CT: comparison of image quality in the detection of colorectal liver metastases. *Radiology* 269(2):469–474. doi:10.1148/radiol.13130002
- Kaza RK, Platt JF, Al-Hawary MM, et al. (2012) CT enterography at 80 kVp with adaptive statistical iterative reconstruction versus at 120 kVp with standard reconstruction: image quality, diagnostic adequacy, and dose reduction. *AJR Am J Roentgenol* 198(5):1084–1092. doi:10.2214/AJR.11.6597
- Flicek KT, Hara AK, Silva AC, et al. (2010) Reducing the radiation dose for CT colonography using adaptive statistical iterative reconstruction: a pilot study. *AJR Am J Roentgenol* 195(1):126–131. doi:10.2214/AJR.09.3855
- Sato J, Akahane M, Inano S, et al. (2012) Effect of radiation dose and adaptive statistical iterative reconstruction on image quality of pulmonary computed tomography. *Jpn J Radiol* 30(2):146–153. doi:10.1007/s11604-011-0026-7
- Katsura M, Matsuda I, Akahane M, et al. (2012) Model-based iterative reconstruction technique for radiation dose reduction in chest CT: comparison with the adaptive statistical iterative reconstruction technique. *Eur Radiol* 22(8):1613–1623. doi:10.1007/s00330-012-2452-z
- Ichikawa Y, Kitagawa K, Nagasawa N, Murashima S, Sakuma H (2013) CT of the chest with model-based, fully iterative reconstruction: comparison with adaptive statistical iterative reconstruction. *BMC Med Imaging* 13:27. doi:10.1186/1471-2342-13-27
- Katsura M, Matsuda I, Akahane M, et al. (2013) Model-based iterative reconstruction technique for ultralow-dose chest CT: comparison of pulmonary nodule detectability with the adaptive statistical iterative reconstruction technique. *Invest Radiol* 48(4):206–212. doi:10.1097/RLI.0b013e31827efc3a

22. Hague CJ, Krowchuk N, Alhassan D, et al. (2014) Qualitative and quantitative assessment of smoking-related lung disease: effect of iterative reconstruction on low-dose computed tomographic examinations. *J Thorac Imaging* 29(6):350–356. doi:[10.1097/RTI.000000000000118](https://doi.org/10.1097/RTI.000000000000118)
23. Yoon HJ, Chung MJ, Hwang HS, Moon JW, Lee KS (2015) Adaptive statistical iterative reconstruction-applied ultra-low-dose CT with radiography-comparable radiation dose: usefulness for lung nodule detection. *Kor J Radiol* 16(5):1132–1141. doi:[10.3348/kjr.2015.16.5.1132](https://doi.org/10.3348/kjr.2015.16.5.1132)
24. Herin E, Gardavaud F, Chiaradia M, et al. (2015) Use of model-based iterative reconstruction (MBIR) in reduced-dose CT for routine follow-up of patients with malignant lymphoma: dose savings, image quality and phantom study. *Eur Radiol* 25(8):2362–2370. doi:[10.1007/s00330-015-3656-9](https://doi.org/10.1007/s00330-015-3656-9)
25. Deak Z, Grimm JM, Treitl M, et al. (2013) Filtered back projection, adaptive statistical iterative reconstruction, and a model-based iterative reconstruction in abdominal CT: an experimental clinical study. *Radiology* 266(1):197–206. doi:[10.1148/radiol.12112707](https://doi.org/10.1148/radiol.12112707)
26. Pickhardt PJ, Lubner MG, Kim DH, et al. (2012) Abdominal CT with model-based iterative reconstruction (MBIR): initial results of a prospective trial comparing ultralow-dose with standard-dose imaging. *AJR Am J Roentgenol* 199(6):1266–1274. doi:[10.2214/AJR.12.9382](https://doi.org/10.2214/AJR.12.9382)
27. Eisenhauer EA, Therasse P, Bogaerts J, et al. (2009) New response evaluation criteria in solid tumours: revised RECIST guideline (version 1.1). *Eur J Cancer* 45(2):228–247. doi:[10.1016/j.ejca.2008.10.026](https://doi.org/10.1016/j.ejca.2008.10.026)
28. Schwartz LH, Bogaerts J, Ford R, et al. (2009) Evaluation of lymph nodes with RECIST 1.1. *Eur J Cancer* 45(2):261–267. doi:[10.1016/j.ejca.2008.10.028](https://doi.org/10.1016/j.ejca.2008.10.028)
29. Wang R, Yu W, Wu R, et al. (2012) Improved image quality in dual-energy abdominal CT: comparison of iterative reconstruction in image space and filtered back projection reconstruction. *AJR Am J Roentgenol* 199(2):402–406. doi:[10.2214/AJR.11.7159](https://doi.org/10.2214/AJR.11.7159)
30. Karpitschka M, Augart D, Becker HC, Reiser M, Graser A (2013) Dose reduction in oncological staging multidetector CT: effect of iterative reconstruction. *Br J Radiol* 86(1021):20120224. doi:[10.1259/bjr.20120224](https://doi.org/10.1259/bjr.20120224)
31. Vardhanabhuti V, Loader RJ, Mitchell GR, Riordan RD, Roobottom CA (2013) Image quality assessment of standard- and low-dose chest CT using filtered back projection, adaptive statistical iterative reconstruction, and novel model-based iterative reconstruction algorithms. *AJR Am J Roentgenol* 200(3):545–552. doi:[10.2214/AJR.12.9424](https://doi.org/10.2214/AJR.12.9424)
32. Yasaka K, Katsura M, Akahane M, et al. (2013) Model-based iterative reconstruction for reduction of radiation dose in abdominopelvic CT: comparison to adaptive statistical iterative reconstruction. *SpringerPlus* 2(1):209. doi:[10.1186/2193-1801-2-209](https://doi.org/10.1186/2193-1801-2-209)
33. European Guidelines on Quality Criteria for Computed Tomography (1999) <http://www.dr.dk/guidelines/ct/quality/index.htm>. Accessed January 2016
34. Olcott EW, Shin LK, Sommer G, et al. (2014) Model-based iterative reconstruction compared to adaptive statistical iterative reconstruction and filtered back-projection in CT of the kidneys and the adjacent retroperitoneum. *Acad Radiol* 21(6):774–784. doi:[10.1016/j.acra.2014.02.012](https://doi.org/10.1016/j.acra.2014.02.012)
35. Nakamoto A, Kim T, Hori M, et al. (2015) Clinical evaluation of image quality and radiation dose reduction in upper abdominal computed tomography using model-based iterative reconstruction; comparison with filtered back projection and adaptive statistical iterative reconstruction. *Eur J Radiol* 84(9):1715–1723. doi:[10.1016/j.ejrad.2015.05.027](https://doi.org/10.1016/j.ejrad.2015.05.027)
36. Vardhanabhuti V, Loader R, Roobottom CA (2013) Assessment of image quality on effects of varying tube voltage and automatic tube current modulation with hybrid and pure iterative reconstruction techniques in abdominal/pelvic CT: a phantom study. *Invest Radiol* 48(3):167–174. doi:[10.1097/RLI.0b013e31827b8f61](https://doi.org/10.1097/RLI.0b013e31827b8f61)
37. Solomon J, Mileto A, Nelson RC, Roy Choudhury K, Samei E (2015) Quantitative features of liver lesions, lung nodules, and renal stones at multi-detector row CT examinations: dependency on radiation dose and reconstruction algorithm. *Radiology* 279:185–194. doi:[10.1148/radiol.2015150892](https://doi.org/10.1148/radiol.2015150892)
38. Thibault JB, Sauer KD, Bouman CA, Hsieh J (2007) A three-dimensional statistical approach to improved image quality for multislice helical CT. *Med Phys* 34(11):4526–4544
39. Solomon J, Mileto A, Ramirez-Giraldo JC, Samei E (2015) Diagnostic performance of an advanced modeled iterative reconstruction algorithm for low-contrast detectability with a third-generation dual-source multidetector CT scanner: potential for radiation dose reduction in a multireader study. *Radiology* 275(3):735–745. doi:[10.1148/radiol.15142005](https://doi.org/10.1148/radiol.15142005)
40. Ramirez-Giraldo JC, Grant KL, Raupach R (2015) ADMIRE: advanced modeled iterative reconstruction (White Paper). Siemens Healthcare